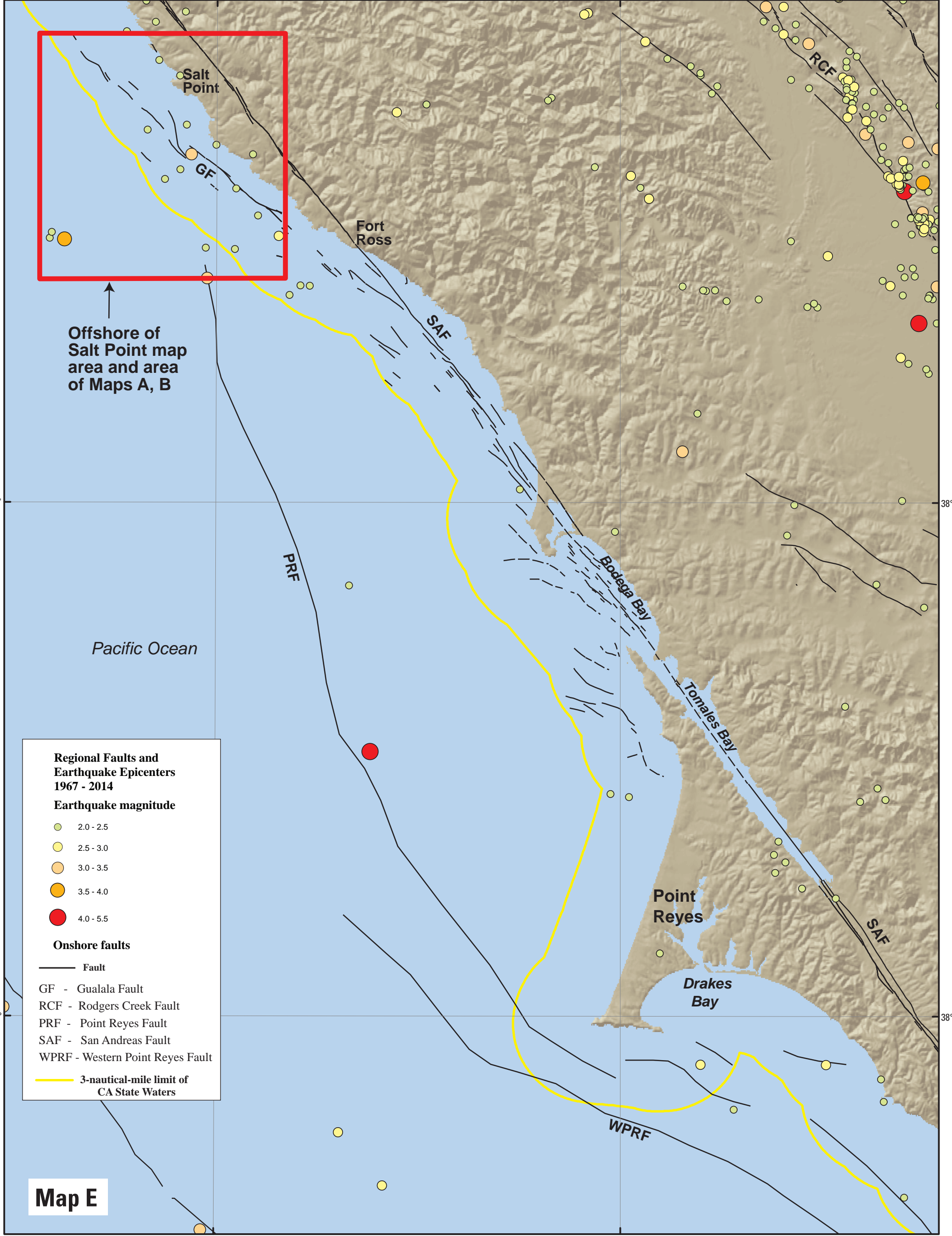
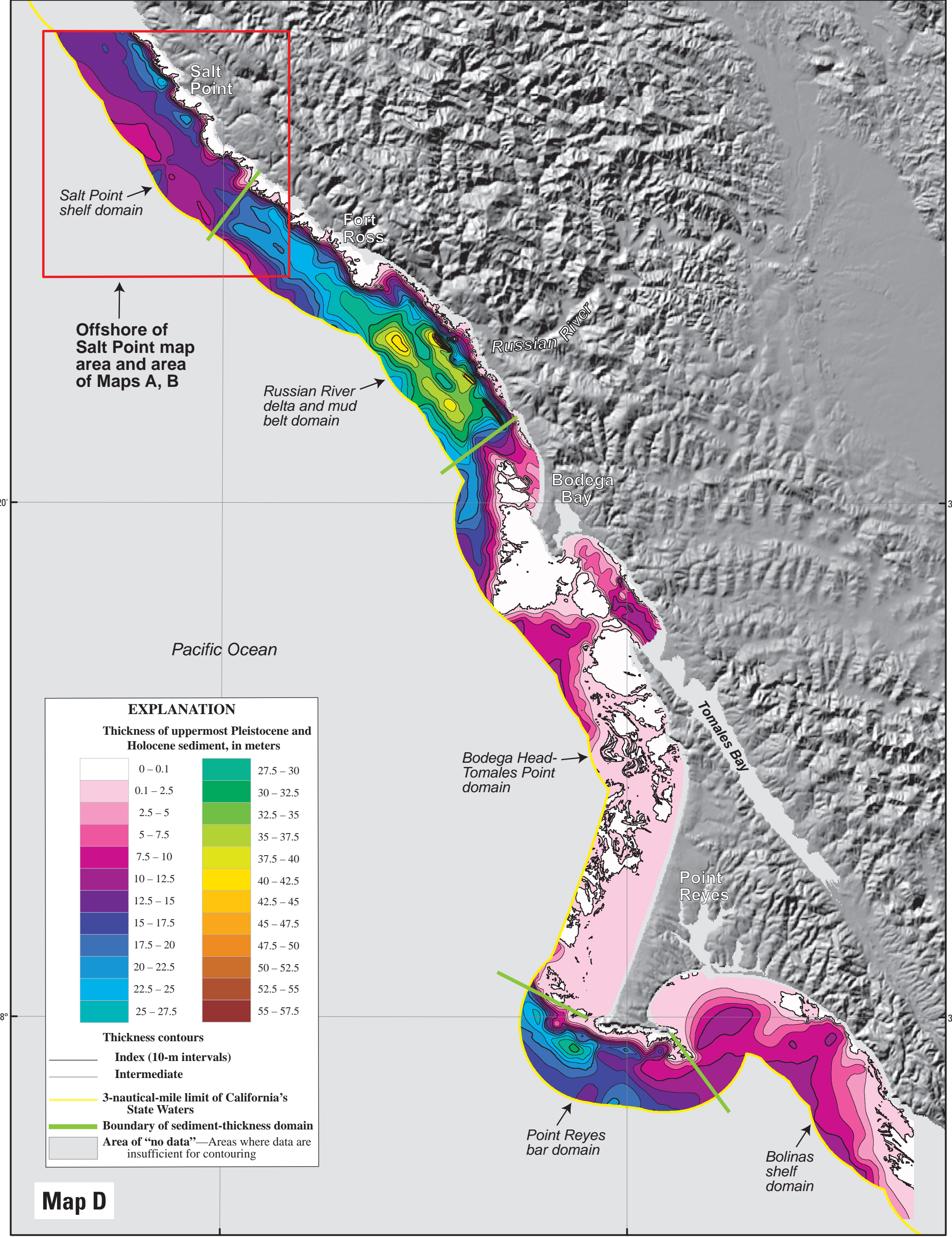
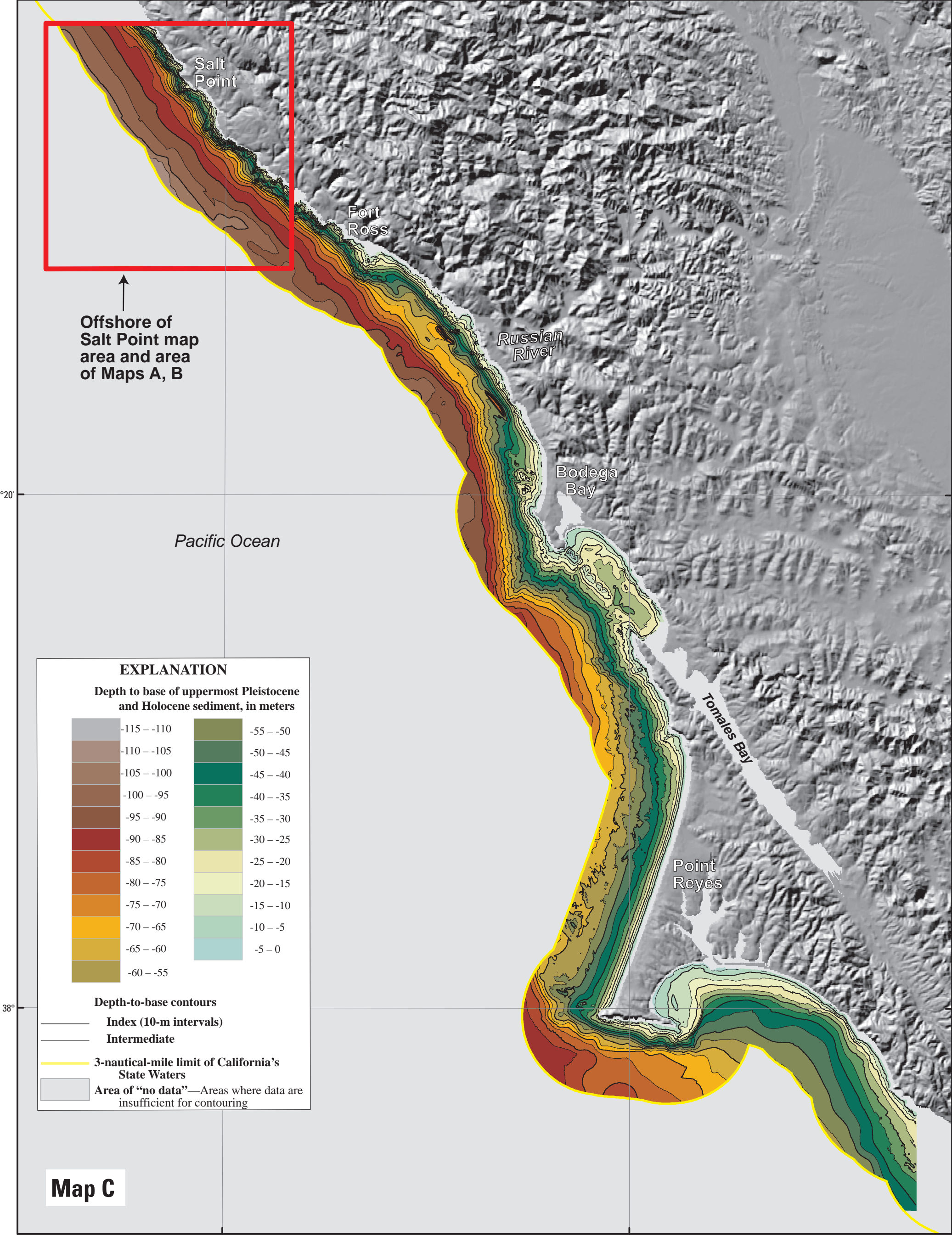


Map A

Map B

Figure 1. USGS high-resolution miniparker seismic-reflection profile PR-121 (collected in 2009 on survey S-8-03-101), which crosses shelf west of Salt Point (see Map A for location), showing faulted and folded strata. Dashed red lines show faults. Magenta symbols show fold axes (dipping arrows, anticlines; converging arrows, synclines). Blue shading shows inferred Pleistocene and Holocene strata, deposited since last sea-level lowstand about 21,000 years ago. Pink shading shows uppermost Pleistocene strata thought to have formed as sea level was falling, between about 30,000 and 21,000 years ago. Thicknesses of these two uppermost stratigraphic units is shown in maps B and D, and depth below sea level to base of these units is shown on maps A and C. Underlying folded reflections are of inferred Pleistocene age. Dashed green lines highlight some continuous reflections that reveal structure (see distinctive stratigraphic markers). Blue dashed lines show low-angle unconformities; dashed purple line is unconformity with Tertiary bedrock. Dashed yellow line is seafloor multiple (see seafloor reflector). Purple triangles show location of California's State Waters limit (yellow line on Map A).

NOT INTENDED FOR NAVIGATIONAL USE



Map C

Map D

Map E

NOT INTENDED FOR NAVIGATIONAL USE

DISCUSSION

This sheet includes maps that show the interpreted thickness and the depth to base of uppermost Pleistocene and Holocene deposits in California's State Waters off the Offshore of Salt Point map area (Maps A, B), as well as for a larger area that extends about 115 km along the coast from Salt Point to Drakes Bay on the south flank of the Point Reyes peninsula (Maps C, D, E) to establish regional context. Uppermost Pleistocene and Holocene deposits in the Offshore of Salt Point map area consist of two units (blue and pink shading in seismic-reflection profile of fig. 1; see also figs. 1, 2, 3, 4, 6, 7, 9, 10 on sheet 8). The stratigraphic position, depth of deposition during a regression (lower pink unit) and subsequent transgression (upper blue unit), with the two units separated by a transgressive surface of erosion (Michaeni and others, 1977; Catusse, 2006). The lower unit is inferred to have formed between about 30,000 and 21,000 years ago (marine isotope stage 2), as sea level fell from about 60 m below present sea level to the Last Glacial Maximum (LGM), approximately 125 to 130 m lower than present (Wachbeck and others, 2002). The upper unit is inferred to have formed during the following transgression. Because this unit and underlying post-LGM deposits each comprise unconsolidated sediments and together overlie a prominent unconformity, our thickness and depth-to-base maps (Maps A, B, C, D) combine these units. To make these maps, water bottom and depth to base of the two upper units horizons were mapped from seismic-reflection profiles. The difference in the two horizons was exported for every shot point as XY coordinates (UTM zone 10) and two-way travel time (TW). The thickness of the two upper units (Maps B, D) was determined by applying a sound velocity of 1,600 m/sec to the TW. The thickness points were interpolated to a preliminary continuous surface, overlaid with zero-thickness bedrock outcrop (sheet 10 of this report), and contoured following the methods outlined in Wong and others (2012). The thickness data points are dense along tracklines (about 1 m apart) and sparse between tracklines (1 km apart), resulting in contouring artifacts. To incorporate the effect of a few rapid thickness changes along faults, to remove irregularities from interpolation, and to represent other geologic information and complexity, the resulting interpolated contours were modified. Contour modifications and regridding were repeated several times to produce the final sediment-thickness maps. Information for the depth to base of the two upper units (Maps A, C) was generated by adding the thickness data to water depths determined by multibeam bathymetry (see sheet 1).

The thickness of the two upper units in the Offshore of Salt Point map area ranges from 0 to 23 m (Map B), and the depth to their base ranges up to about 107 m (Map A). Mean sediment thickness for the map area is 12.1 m and total sediment volume is 1.226 × 10⁶ m³. Most of the seafloor within about 1 km of the shoreline (water depths of about 30 to 50 m) consists of bedrock outcrop with little or no sediment cover except in a few areas at the mouths of coastal watersheds such as Miller Creek (pamphlet, fig. 1-2) on the north flank of Salt Point (Maps A, B), where fluvial channels eroded through bedrock during late Quaternary sea-level lowstands.

There are two notable zones of increased sediment thickness in the map area (Map B). The first, forms an about 1-km-wide, shore-parallel zone north of Salt Point at water depths of about 50 m. Thickness in this zone largely results from the presence of a downlapping sediment wedge (pink shaded unit on fig. 1) that accumulated along the southwest flank of the nearshore bedrock (Map A, fig. 1; also see figs. 2, 3, 4, on sheet 8). Subparallel to diverging reflections within this sediment wedge (only bedrock to the northeast and downlap folded sediments to the southwest). This wedge is inferred to consist primarily of relatively coarse-grained sediments (sheet 10) derived from local watersheds with the highest sediment accumulation rates occurring about 30,000 to 21,000 years ago when this zone occupied the nearshore during the last sea-level fall.

The second notable zone of increased sediment thickness (Map B) forms an about 2-km-wide, shore-parallel zone in the southeastern part of the map area at water depths of about 60 to 85 m. This zone, northeastern part of this second zone occurs in an area of fine-grained surface sediments, a "mud belt" derived from the Russian River, which enters the Pacific Ocean about 15 km southeast of the map area (Map C; Kline, 1984; Drake and Cushman, 1985). The Russian River has a very large sediment load (estimated 900,000 metric tons/yr; Farnsworth and Warwick, 2007) and the increased sediment thickness in this mudbelt area is associated with significant sediment supply from this source. Local coastal watersheds are significantly less important sediment sources. These watersheds extend just 2 to 3 km east from the shoreline and their role as sediment sources diminished during sea-level rise as the seaward portions of their drainage basins became submerged.

Five different "domains" of sediment thickness are recognized on the regional sediment-thickness map (table 7-1 in pamphlet; Map D), each with distinctive geologic controls: (1) The Salt Point shelf domain, located in the far western part of the map area, has a mean sediment thickness of 11.7 m. The thickest sediment (20 to 25 m) is found where a pre-LGM, regressive, downlapping sediment wedge formed above a break in slope that is controlled by a contact between harder bedrock and softer, folded, Pleistocene sediments in this domain. Sediment thinning in this domain in the more proximal California's State Waters is the result of a relative lack of sediment supply from local watersheds, as well as a more distal Russian River source. (2) The Russian River delta and mud belt domain, located offshore of the largest sediment source on this part of the coast, has the thickest uppermost Pleistocene and Holocene sediment in the region (mean thickness, 21.1 m). The northeastward extension into the mudbelt "mud belt" results from onshore shelf bottom sediment transport (Drake and Cushman, 1985). This domain includes a section of the San Andreas Fault Zone (Map E), which here is characterized by several releasing, right-stepping strands that bound narrow, elongate, pull-apart basins; these sedimentary basins contain the greatest thickness of uppermost Pleistocene and Holocene sediment (about 50 m) in the region. (3) The Bolinas Head-Tomales Point shelf domain, located between Bolinas Head and the Point Reyes headland, contains the least amount of sediment in the region (mean thickness, 3.4 m). The lack of sediment results from decreased "accommodation of sediment" (note shallow depth contours on Maps A and C) and limited sediment supply. (4) The Point Reyes bar domain, located west and south of the Point Reyes headland, is a local zone of increased sediment thickness (mean thickness, 14.3 m) more proximal to the Point Reyes headland during rising sea level. (5) The Bolinas shelf domain, located east and southeast of the Point Reyes headland, has a thin sediment cover (mean thickness of 5.6 m), which likely results from limited sediment accumulation space caused by tectonic uplift water depths in this domain within California's State Waters are less than 45 m, as well as limited sediment supply and the high wave energy that is capable of reworking and transporting shelf sediment to deeper water.

Map E shows the regional pattern of major faults and of earthquakes occurring between 1967 and April 2014 that have inferred or measured magnitudes of 2.0 and greater. Fault locations, which have been simplified, are compiled from our mapping within California's State Waters (see, for example, sheet 10) and the Quaternary fault and fold database (U.S. Geological Survey and California Geological Survey, 2010). Earthquake epicenters are from the Northern California Earthquake Data Center (NCEDEC), which is maintained by the U.S. Geological Survey and the University of California, Berkeley, Seismological Laboratory. The largest recorded earthquake in the map area (M3.7, 7/6/2006) occurred about 13 km offshore. There has been a notable lack of microseismicity on the adjacent San Andreas Fault since the devastating great 1906 California earthquake (M7.8, 4/18/1906), thought to have nucleated on the San Andreas Fault offshore of San Francisco (see, for example, Bolt, 1988; Leonard, 2005), about 100 km south of the map area.

REFERENCES CITED

Bolt, B.A., 1988. The focus of the 1906 California earthquake. *Bulletin of the Seismological Society of America*, v. 58, p. 457-471.

Catusse, O., 2006. Principles of sequence stratigraphy. *American, Elsevier*, 375 p.

Drake, D.E., and Cushman, D.A., 1985. Seasonal variation in sediment transport on the Russian River shelf, California. *Continental Shelf Research*, v. 4, p. 695-714. doi:10.1016/0278-4328(85)90007-X.

Farnsworth, K.L., and Warwick, J.A., 2007. Sources, dispersal, and fate of fine sediment supplied to coastal California. *U.S. Geological Survey Scientific Investigations Report 2007-5254*, 77 p., available at <http://pubs.usgs.gov/ofr/2007/5254/>.

Kline, D.L., 1984. Modern sedimentation on the California continental margin adjacent to the Russian River. M.S. thesis, San Jose State University, 120 p.

Lomas, A., 2005. A reanalysis of the hypothetical location and related observations for the Great 1906 California earthquake. *Bulletin of the Seismological Society of America*, v. 95, p. 861-877. doi:10.1785/B0120040141.

Michaeni, R.M., Jr., Vail, P.R., 1977. Seismic stratigraphy and global changes of sea level part 6—Stratigraphic interpretation of seismic reflection patterns in depositional sequences. In Payton, C.E., ed., *Seismic stratigraphy—Applications to hydrocarbon exploration*. Tulsa, Oklahoma, American Association of Petroleum Geologists, p. 117-135.

Northern California Earthquake Data Center, 2014. Northern California earthquake catalog: Northern California Earthquake Data Center database, accessed April 5, 2014, at <http://www.ncedec.org/ncsa/>.

Pelster, W.R., and Fairbanks, R.G., 2006. Global glacial ice volume and Last Glacial Maximum duration from an extended Barbados sea level record. *Quaternary Science Reviews*, v. 25, p. 3,323-3,377. doi:10.1016/j.quascirev.2006.04.010.

U.S. Geological Survey and California Geological Survey, 2010. Quaternary fault and fold database of the United States. U.S. Geological Survey database, accessed April 5, 2014, at <http://earthquake.usgs.gov/hazards/gfandf/>.

Wachbeck, C., Labeyrie, L., Michel, E., Duplessy, J.C., McManus, J.F., Labeyrie, M., Balbon, E., and Labeyrie, M., 2002. Sea-level and deep-water temperature changes derived from benthic foraminifera isotopic records. *Quaternary Science Reviews*, v. 21, p. 295-305.

Wong, F.L., Phillips, E.L., Johnson, S.Y., and Siller, R.W., 2012. Modeling of depth to base of Last Glacial Maximum and seafloor sediment thickness for the California State Waters Map Series, eastern Santa Barbara Channel, California. *U.S. Geological Survey Open File Report 2012-1161*, 16 p., available at <http://pubs.usgs.gov/ofr/2012/1161/>.